

pubs.acs.org/jchemeduc Demonstration

## Using Magnets and Flexible 3D-Printed Structures to Illustrate <sup>2</sup> Protein (Un)folding

3 Ionel Popa\* and Florin Saitis



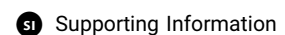
Cite This: https://doi.org/10.1021/acs.jchemed.2c00231

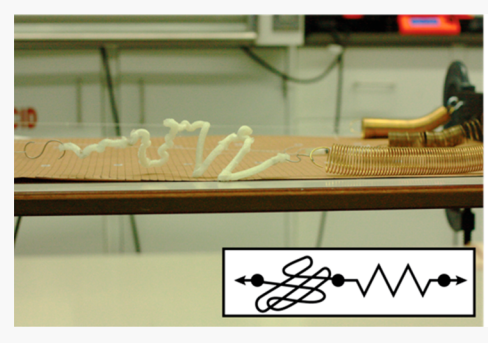


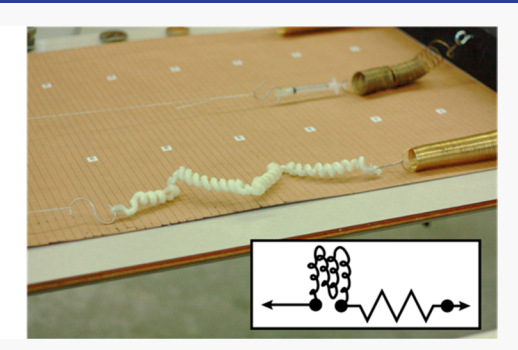
ACCESS I

Metrics & More









4 ABSTRACT: Proteins are "magical" workers inside our body, as they accomplish most of the cellular functions. Here we report on a 5 novel approach to teach protein folding and unfolding, using magnets and flexible 3D-printed protein structures. To illustrate this 6 physical process, we used colored circular magnets designed for whiteboards, connected through paper clips. Several protein 7 structures were then 3D-printed, using both standard and flexible materials. Protein unfolding under force was then investigated by 8 adding slotted weights to a setup consisting of three experiments: a simple spring, a spring in series with a sealed syringe 9 (representing a dashpot), and a spring in series with a printed protein structure. All of the experiments shown here were done as part 10 of the event, organized by the University of Wisconsin—Milwaukee. The approach presented here complements the use of other 11 techniques to learn about protein folding and constitutes a novel way to explain how mechanical unfolding in vivo relates to a gain-of-12 function.

13 KEYWORDS: Protein Structure, Protein Folding, Mechanical Unfolding of Proteins, 3D-Printing of Flexible Structures

### INTRODUCTION

15 Proteins are molecular machines that carry out the majority of 16 biological functions, from catalyzing reactions and providing 17 structural support to acting as nanometric-sized motors. In 18 order for proteins to perform their function in vivo, they first 19 need to acquire a specific 3-dimensional (3D) structure. This 20 process of a polypeptide chain acquiring a specific structure 21 based on a given amino acid sequence is known as protein 22 folding and still represents one of the open questions in 23 science.<sup>2</sup>

Cells represent the smallest structural unit of our body that 25 can self-replicate. Our genetic information is stored inside the 26 nucleus in the form of DNA, which itself is divided into 27 chromosomes. Each of the over 20,000 proteins in the human 28 body has a corresponding section in the genome encoding for 29 it, known as a gene. The DNA encodes this information via its 30 nucleotide sequence, which has in its structure cytosine [C], guanine [G], adenine [A], or thymine [T] nitrogen-containing 32 bases. Through the process of transcription, the sequence 33 encoding for a specific protein is assembled into an mRNA 34 (mRNA) molecule, which has the same C, G, and A 35 nucleotides, while T is replaced by uracil [U]. mRNA may

then exit the nucleus to become the template for protein 36 synthesis through translation. During translation, the ribosome 37 decodes the mRNA sequence a codon (3 base pairs) at a time 38 to produce a polypeptide with a well-defined sequence, made 39 from a total of 20 amino acids.

There are also several distinct organization levels for protein 41 structure. The first level is the primary structure, which is 42 given by the sequence of amino acids forming the protein 43 backbone. The secondary structure of proteins has two main 44 elements,  $\alpha$ -helices and  $\beta$ -strands (or sheets).  $\alpha$ -Helices form 45 between adjacent amino acids, while  $\beta$ -strands appear between 46 parts of the protein sequence that can even be at opposite 47 ends. The tertiary structure of a protein, also known as the 48 native state, represents a relatively well-defined stable 3D 49 arrangement of secondary structure elements and unstructured 50

Received: March 15, 2022 Revised: June 14, 2022



Journal of Chemical Education pubs.acs.org/jchemeduc Demonstration

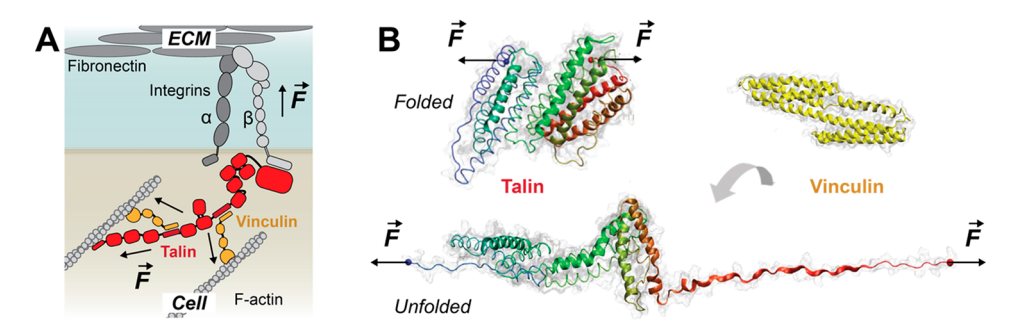


Figure 1. Schematics of how protein unfolding under a force vector represents a mechanically induced signaling mechanism. (A) Schematics of the first steps during the formation of focal adhesions, which are mechanical connections between cells and their extracellular matrix (ECM). Talin unfolding of its tail domains (red) allows for the formation of new connections with actin cytoskeleton via vinculin (orange), as force develops via the integrin-extracellular matrix (fibronectin) pathway. Adapted with permission from ref 7. Copyright 2020 John Wiley and Sons. (B) Molecular representation of the unfolding-induced binding process of vinculin to talin, derived from crystal structures and from molecular dynamics simulations. Top left: Folded talin domains. Bottom: Same domains being mechanically unfolded to expose vinculin binding sites. Adapted with permission from ref 8. Copyright 2009 The American Association for the Advancement of Science.

51 regions. Some proteins also have quaternary structures, which 52 are made either through the assembly of several repeats of the 53 same domain (homomers) or assemblies with other proteins 54 (heteromers). The tertiary and quaternary structures play the 55 most important role in the function of proteins. As discussed 56 below, in some cases, the unfolding and refolding of the native 57 structure also influences the function of some proteins in vivo. The process of protein folding entails the transition from the primary to the tertiary structure and is both fascinating and 60 inherently complex. An average polypeptide chain has a 61 staggering number of possible conformations that it could 62 adopt. As proteins typically fold within a few milliseconds, 63 most of these possible conformations are not being sampled, 64 and the folding process is somehow guided.<sup>3</sup> There are several 65 important steps driving protein folding, which can be divided 66 on the basis of their timing and complexity: entropic collapse, 67 hydrophobic collapse, formation of secondary structure elements, and molten globule formation. During entropic collapse, the reduction in dimensionality occurs because it is 70 more energetically favorable for a polymer (or peptide chain) 71 to adopt a collapsed rather than a stretched conformation. Throughout the hydrophobic collapse, amino acids rearrange themselves such that the hydrophilic amino acids form the shell and the hydrophobic amino acids the core of the 75 structure. This process is typically preceded by the formation of  $\alpha$ -structure elements and followed by the expulsion of water 77 molecules (known as the "dry" molten globule state<sup>6</sup>). Following the formation of  $\beta$ -strands, the protein acquires its 79 native 3D folded structure. In one of the demonstrations 80 shown in this study, we focus on the hydrophobic collapse step 81 of protein folding.

Recently, experimental evidence has surfaced that suggests that some proteins unfold and refold *in vivo* as a novel and yet poorly understood phenomenon. We refer the reader to a review on this process, where sequential unfolding and refolding of protein domains produces some interesting gain-of-function effects, such as adaptive changes in elasticity, storage, and release of mechanical energy, and exposure of buried binding sites, of disulfate bonds or other amino acids that could be posttranslationally modified. Here we will discuss only one such example.

Cells continuously exchange mechanical cues with them-93 selves and their extracellular matrix (ECM), and this 94 interaction determines if a cell will function normally, or

undergo division, or even die by apoptosis. 1,9 When interacting 95 with their ECM, cells form focal adhesions, where their 96 cytoskeleton is rearranged to allow for movement and to match 97 developing extracellular forces. This complex process is 98 controlled by a protein named talin, which effectively 99 represents a molecular mechanical computer (Figure 1). 100 fl Talin can attach between an actin filament and a trans- 101 membrane integrin complex. As the integrin complex binds to 102 an extracellular ligand, it can generate more and more pulling 103 force (Figure 1A). So, how do cells match these developing 104 pulling forces? Like in a tug-of-war, talin tail domains unfold 105 and can expose up to 11 previously hidden (cryptic) binding 106 sites for another protein called vinculin (Figure 1B).8 Vinculin, 107 in turn, can recruit more actin filaments, forming a branched 108 structure and distributing the developing forces. In the second 109 part of this paper, we will focus on how tethered proteins can 110 unfold and refold under a changing force vector. These 111 mechanically controlled processes are currently poorly under- 112 stood but may play a yet to be fully recognized role on how 113 proteins integrate mechanical signaling.

Hands-on experiments have been shown to improve 115 students' understanding, 10,11 and the use of 3D-printing is 116 becoming an increasingly useful approach toward learn- 117 ing. 12-14 Here we report the use of magnets and 3D-printed 118 structures to illustrate details related to protein (i) folding, (ii) 119 structure, and (iii) unfolding under a force vector. These 120 processes follow the chronological events in the life of a 121 protein inside our cells. All of the experiments shown here 122 were performed as part of an event organized by the author 123 with the help of his host institution. This event aimed to attract 124 a young audience (K-12) to STEM by demonstrating various 125 protein foldings through hands-on experiments. The event was 126 repeated 5 times during the month of January 2022 and had a 127 total audience of 143 people. The approach presented here 128 complements the use of other techniques to learn about 129 protein folding 15-19 and constitutes a novel way to explain 130 how mechanical unfolding *in vivo* relates to a gain-of-function. 131

## Illustrating Protein Folding with Connected Magnets

Here we first aim to illustrate how a polypeptide chain can reduce 133 its number of possible conformations through the segregation of 134 hydrophobic and hydrophilic amino acids, also known as the 135 hydrophobic collapse. Following translation, the emerging 136 polypeptide chain exits the ribosome to encounter water 137 molecules, as well as folding helpers, known as chaperones. 138

#### **HYDROPHILIC AMINO ACIDS**

#### HYDROPHOBIC AMINO ACIDS

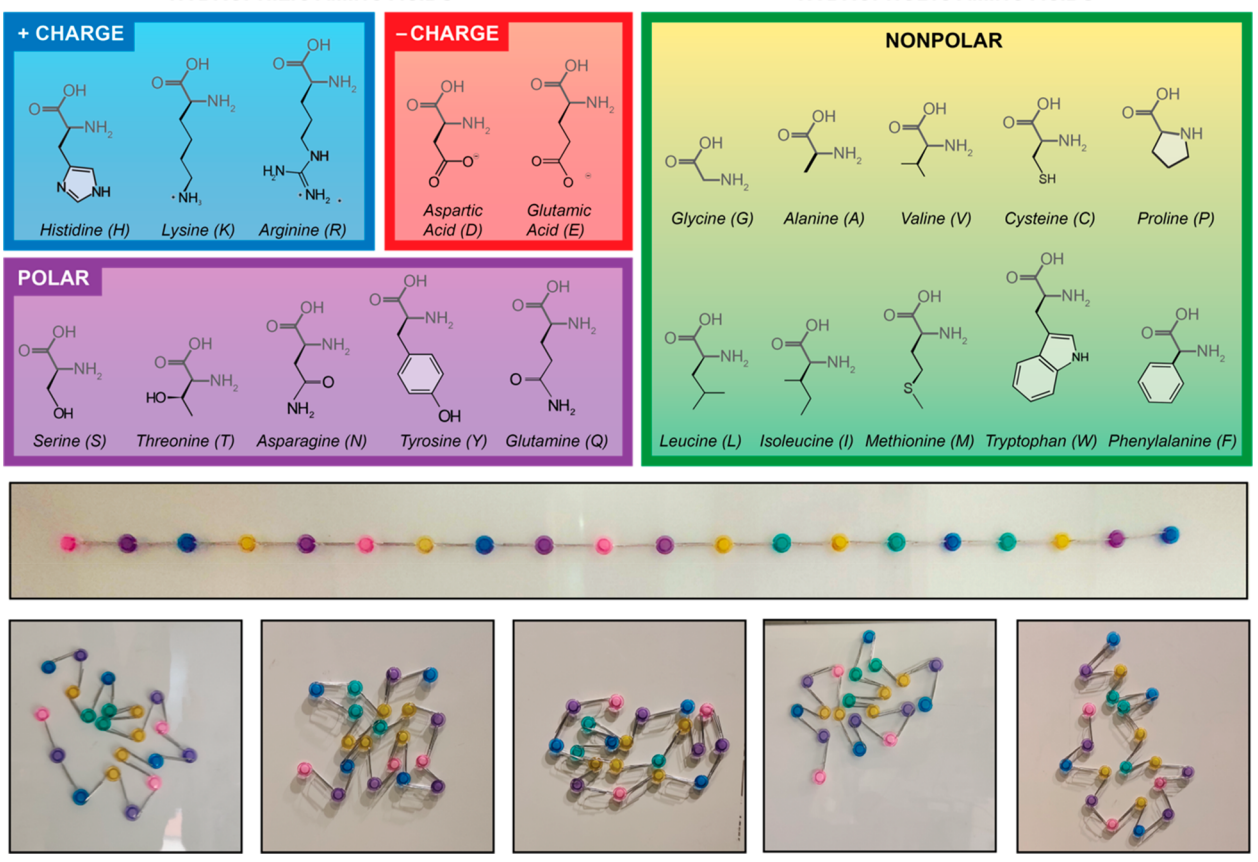


Figure 2. Illustrating hydrophobic—hydrophilic segregation during protein folding. (Top) Structure of the 20 amino acids found in proteins, grouped as positively charged (blue), negatively charged (red), polar (purple), and nonpolar (yellow-green). The charged and polar amino acids are hydrophilic, while the nonpolar amino acids are water hydrophobic. (Middle) Magnets following the same color code arranged in a random sequence and connected with paper clips, representing a stretched amino acid chain. (Bottom) Five arrangements done by participants at the event, who were asked to collapse the stretched sequence such that the hydrophobic amino acids form the core and the hydrophilic amino acids the shell. Note: As the kits come with an equal number of colored magnets, to minimize costs we chose to represent the hydrophobic amino acids with two colors (green and yellow), without making a distinction between these two colors.

139 There are a total of 20 amino acids that can be viewed on the 140 basis of their interaction with water (Figure 2A, top). Half of 141 these amino acids can be classified as hydrophilic and half as 142 hydrophobic. The hydrophilic amino acids can be divided into 143 three categories: positively charged (marked in blue), 144 negatively charged (marked in red), and polar, having 145 asymmetric charge distribution but no free charge (marked 146 in purple). As the amino acids chain emerges from the 147 ribosome, the hydrophobic ones will minimize their interaction 148 energy by clustering away from the solvent, inside the core of 149 the molecule, while the hydrophilic amino acids will go to form "protective" shell. Furthermore, amino acids with a similar 151 charge will tend to move away from each other, while 152 oppositely charged amino acids will attract each other. To 153 illustrate this physical process, we used circular magnets 154 designed for whiteboards, which come in sets of 60 pieces and 155 five colors (bought from Toodoo Cat. No. 44111900, via 156 Amazon). Two holes were made at opposite ends of these 157 magnets, which were then connected using paper clips (Figure 158 2, middle). The magnets were then arranged in random 159 sequences, and 3 chains representing 3 different amino acid 160 sequences were assembled. During the event, the students were 161 asked to collapse the magnet-chains following the rules that 162 yellow and green magnets should not be exposed to the 163 environment, while blue, red, and purple should. Furthermore,

f2

red-red and blue-blue magnets should not be in close 164 proximity, while red-blue should. Figure 2, bottom, and 165 Figure S1 show five arrangements done by participants at the 166 event following the instructions above. The students were also 167 asked to have the shortest distance between the magnets larger 168 than one paper clip length. While using the exact same magnet 169 sequence, five different collapsed structures were obtained. We 170 noticed that most of the students had in the beginning a hard 171 time working out a procedure to move around the magnets 172 and match the interactions. However, once the students were 173 told to focus on having the hydrophobic amino acids inside the 174 structure (the yellow and green magnets pointing toward the 175 center), they managed to find functional conformations right 176 away. The organizers also advised the students toward the end 177 of the experiment to try to have only magnets representing 178 charged and polar amino acids exposed to the surroundings, to 179 avoid having positive-positive charges (blue-blue magnets) 180 or negative-negative charges (red-red magnets) adjacent to 181 each other, and to try to have positive-negative charges 182 (blue-red magnets) close together. In some experiments, 183 there were still some yellow/green magnets exposed, and some 184 magnets were closer than a paper clip length. The students 185 learned that a long polypeptide chain becomes a collapsed 186 structure based on the interaction of amino acids with water. 187 This experiment clearly shows how, based on their interaction 188

198

199

200

201

202

203

204

205

206

207

208

209

210

211

212

213

214

215

216

217

218

219

220

221

222

223

224

225

226

227

228

229

230

231

232

233

234

235

236

237

238

239

240

241

242

243

189 with water and with themselves, amino acids can collapse to 190 reduce their dimensionality.

## 191 Using 3D-Printing to Visualize Folded Structure of

193 To illustrate the diversity and beauty of folded proteins, we 194 chose to 3D-print some representative structures. 3D-printing 195 of proteins was reported previously, 20–22 and our protocol was 196 adapted from these studies. Briefly, the steps that were 197 followed were the following:

- 1. A. pdb file (which is a textual file format describing the three-dimensional coordinates of amino acids for a folded protein, stored in the Protein Data Bank) was downloaded and saved on the desktop. In the case of structures made with several domains or crystal structures with multimeric molecules, only a single domain was kept, and the .pdb file resaved, using molecular visualization software (such as PyMOL available at https://pymol.org/2/).
- 2. The .pdb file can then be opened in molecular visualization software that is capable of exporting in the .stl format, such as Visual Molecular Dynamics (VMD), available at http://www.ks.uiuc.edu/Research/vmd/, or Chimera, available at https://www.rbvi.ucsf.edu/chimera/. Since the structures generated with VMD produced more cylindrical representations, which printed better, the remainder of this procedure will describe the steps needed to be taken for VMD.
- 3. Following the loading of a structure in VMD, we chose Secondary Structure under Coloring Method, and New Cartoon under Drawing Method. We also changed the Aspect Ratio to 1.0, the Thickness to 1.65, and the Resolution to 50. From the Display menu, we then removed the Axes (Off) from being displayed and changed the perspective to Orthographic. The structure was then rendered as an .stl file from the File menu.
- 4. The files were then imported in the *Ultimaker Cura* 3D slicer. Here they were scaled to the desired size. First, the presetting for the used filament was loaded (in our case either *PLA—polylactic acid* or *TPU—thermoplastic polyurethane*). The printing temperature was further adjusted to follow the filament manufacturer specifications. The *Infill Density* was set to 50%, and the layer thickness to 0.3 mm. *Generate Support* was selected having *Tree* as *Support Structure* and the *Support Placement* as *Touching Buildplate*. We recommend Cura as opposed to the Prusa slicer, as it allows generation of tree-supports, that produce prints which are easier to clean.
- 5. All structures were printed using a Prusa i3MK3S+ 3D-printer (Prusa Research), equipped with a 0.4 mm nozzle. The names of the used filaments are provided in the description of each print. Following the print, the tree-supports were carefully removed with a plier.
- 6. (Optional) Printed proteins can be painted with acrylic colors to underline various structural elements (see Supporting Information Figure S2).

One print is of the bacterial protein L (pdb code 1hz6; 246 Figure 3A). This simple  $\alpha$ – $\beta$  protein is ideal for showing 247 various secondary structure elements. *In vivo*, several domains 248 of protein L are secreted by streptococcus bacteria to target 249 antibodies. We chose this protein, as it has been extensively 250 studied as a model protein for folding  $^{24,25}$  and is one of the

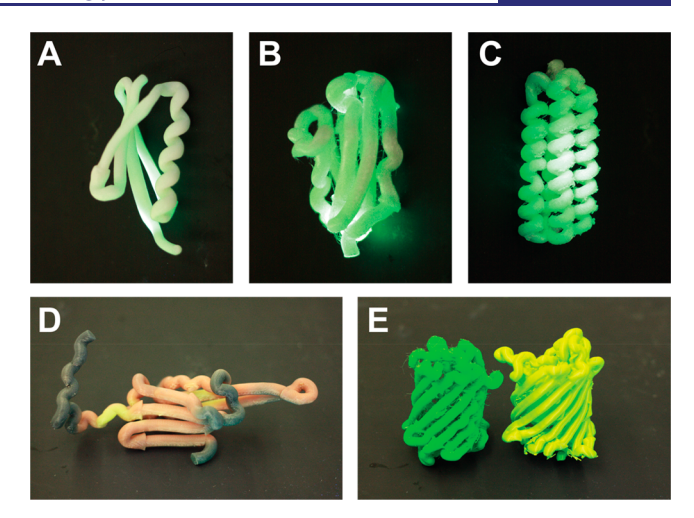


Figure 3. 3D-prints of proteins. (A) Bacterial protein L, printed in glow in the dark PLA. (B) Titin I10, printed in TPU. (C) Talin R9, printed in TPU. (D) Crystallin, printed in Color Changing with Temperature PLA. (E) GFP, printed in Green Flexible PLA Plus and Shiny Lime Green Silk PLA.

rare cases where the bacterium, which typically is the "prey" for 251 our immune system, becomes the "predator", targeting 252 antibodies in order to disrupt the immune response. We 253 chose to print it using Glow in the Dark PLA Filament 254 (Hatchbox), which glows green in the dark and can also be 255 easily painted on.

Another protein, crystallin (pdb code 3l1e), was printed 257 using Tri Color Changing with Temperature PLA Filament 258 (Amolen Tech). Crystallin is part of the cornea and the lens of 259 our eyes. Tather ironically, when present in low concentrations, as is the case in most of our cells, this protein prevents 261 other proteins from forming crystals and aggregates. In this 262 capacity, it is known as a heat-shock protein, which is 263 expressed when the body temperature rises. To illustrate the 264 role of crystallin to mitigate cellular stress, as it performs 265 chaperone functions and helps other proteins fold correctly, as 266 the body temperature rises, we chose a PLA that changes color 267 with temperature. Using a heat-blower, the printed structure 268 can be exposed to temperatures equal to or higher than the 269 body temperature, turning its color from black to red or yellow, 270 respectively (Figure 3B).

The proteins in Figure 3C,D represent the I10 domain of 272 titin (from PDB code 5jde), and the R9 domain of talin (pdb 273 code 2kbb), respectively. They were printed using Glow in The 274 Dark Luminous Green TPU (from SainSmart). As mentioned 275 in the Introduction, titin, the largest protein in the human 276 body, is made of up to 100 folded domains and two spring-like 277 unstructured regions.<sup>28</sup> Titin acts as both a biological spring 278 and an active participant in muscle contraction by continuously 279 unfolding and refolding some of its Immunoglobulin (Ig)-like 280 domains, such as I10 (Figure 1A). Talin, as well, operates 281 under a force vector and unfolds its rode domains to expose 282 binding sites and drive focal adhesion formation (Figure 1B). 283 While both proteins operate in a similar way, they have vastly 284 different structures, with titin domains being mostly  $\beta$ -strands, 285 and talin domain having only  $\alpha$ -helices. The proteins printed in 286 TPU can be unfolded and extended and were further used to 287 demonstrate protein unfolding.

Another protein that we chose to print is green fluorescence 289 protein (GFP, Figure 3E; pdb code 4kw4). This protein 290

Journal of Chemical Education pubs.acs.org/jchemeduc Demonstration

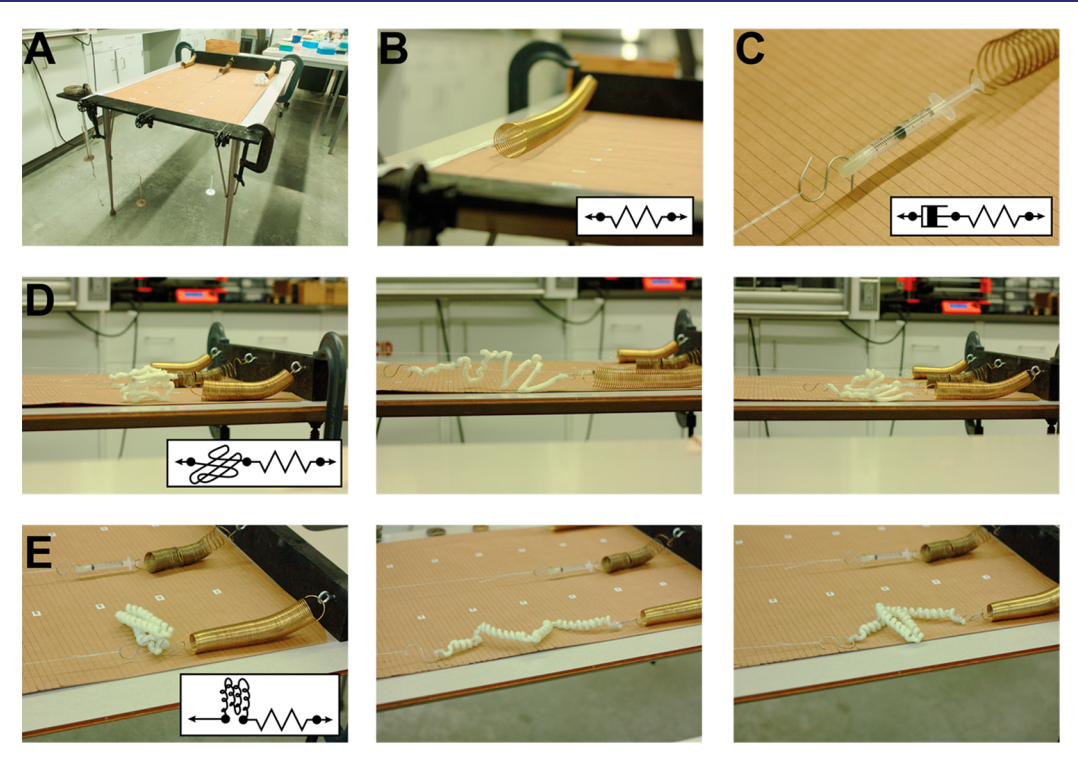


Figure 4. Simple setup to demonstrate how spring, dashpots, and proteins respond to mechanical forces. (A) Picture of the overall setup, reassembled in our lab, showing the three main components, as well as the general assembly. (B) Picture of a spring under force, extending proportionally. (C) Picture of a spring in series with a syringe. Over a certain range of forces, the syringe plunger slowly moves, representing the viscoelastic response of a dashpot. (D) Pictures of a muscle titin I10 domain in series with a spring. (E) Pictures of a talin R9 domain in series with a spring. For both panels D and E, left, snapshot is at a low force (before the protein domain unfolds), middle, at a higher force (following unfolding) and, right, back at a lower force (where both the spring and protein contract, but before domain refolding).

291 discovered in jellyfish is extensively used by scientists as a 292 molecular reporter. <sup>29</sup> When exposed to the blue or ultraviolet 293 (UV) light, GFP glows bright green. Many other variants were 294 developed that produce other colors (which have different 295 emission spectra). GFP has an interesting  $\beta$ -barrel structure 296 and was printed in a Shiny Lime Green Silk PLA filament 297 (Polymaker). As this filament was quite brittle and GFP has a 298 very complex structure that is hard to remove supports, we also 299 printed it using Green Flexible PLA Plus (Ataraxia Art). When 300 talking about GFP, purified solutions of various variants, from 301 blue to red, were shown under a UV light, to demonstrate their 302 fluorescence.

# 303 Mechanical Unfolding Experiment Using Springs and 304 3D-Printed Flexible Structures

305 There is a profound, yet poorly understood, physics behind 306 how protein unfolding under a force vector affects the overall 307 extension and elasticity of cells and tissues. Unfolding of a 308 protein domain results in a sudden increase in the overall 309 contour length, and it looks like a spring being instantaneously 310 added or subtracted over/under a certain force. To make 311 things even more complicated, at the single molecule level, the 312 process is probabilistic (and not deterministic), meaning that 313 the same protein domain at the same pulling force will take 314 some finite amount of time to unfold.<sup>30</sup> This time will be 315 slightly different if the experiment is repeated over and over 316 again and depends on the local interactions between the 317 domain and the solvent molecules, as well as on the continuous 318 formation and breaking of hydrogen bonds inside the protein 319 structure. This addition and subtraction of contour length as 320 the force changes, in the context of tens-to-thousands of 321 domains in series, increases the extension range and response

time of a molecule without significant variations on the force- 322 per-molecule. This process provides, for example, a large range 323 of operating conditions for our muscles, <sup>28,31</sup> which can be stiff 324 while we stand, as most domains can be folded, and elastic 325 when we exercise, as some domains may unfold. To illustrate 326 this process, we designed a setup that shows how a spring, a 327 dashpot, and a protein domain respond to changing forces. A 328 dashpot is a damper used to describe time-dependent motions. 329 Our setup consisted of a ledge clamped on a table, with three 330 components (Figure 4A). A first component had a spring 331 f4 attached to the ledge in series with a string that was passed 332 over a wheel and connected to a weight hanger (parts bought 333 from Pasco) (Figure 4B and Movie S1). The second 334 component had a spring in series with a 3 mL syringe 335 (Teleflex), followed by the same wheel-weight hanger setup. 336 The syringe had a 3D-printed plunger at its end, to seal it 337 (printed in TPU, see design file in Supporting Information) 338 (Figure 4C and Movie S2). A larger syringe (20 mL), with its 339 end sealed with a finger, was shown to demonstrate that when 340 the force is released, the plunger slowly moves back due to the 341 vacuum force. The third component had a spring in series with 342 a 3D-printed protein structure (in TPU) (Figure 4D,E, and 343 Movie S3 and Movie S4). The protein had at its mechanical 344 clamp, which for both titin I10 and talin R9 is between the first 345 and last structural elements, glued magnets (N52, K&J 346 Magnetics). These magnets were inserted in holes predrilled 347 at the opposite sides and glued with epoxy glue. Magnets are 348 ideal to represent the hydrogen bonds that hold together the 349 protein structure, as they have a strong attractive interaction, 350 which is relatively short-ranged. For the protein structure, the 351 metal weight hanger (which weight ~50g) was replaced with a 352

Journal of Chemical Education

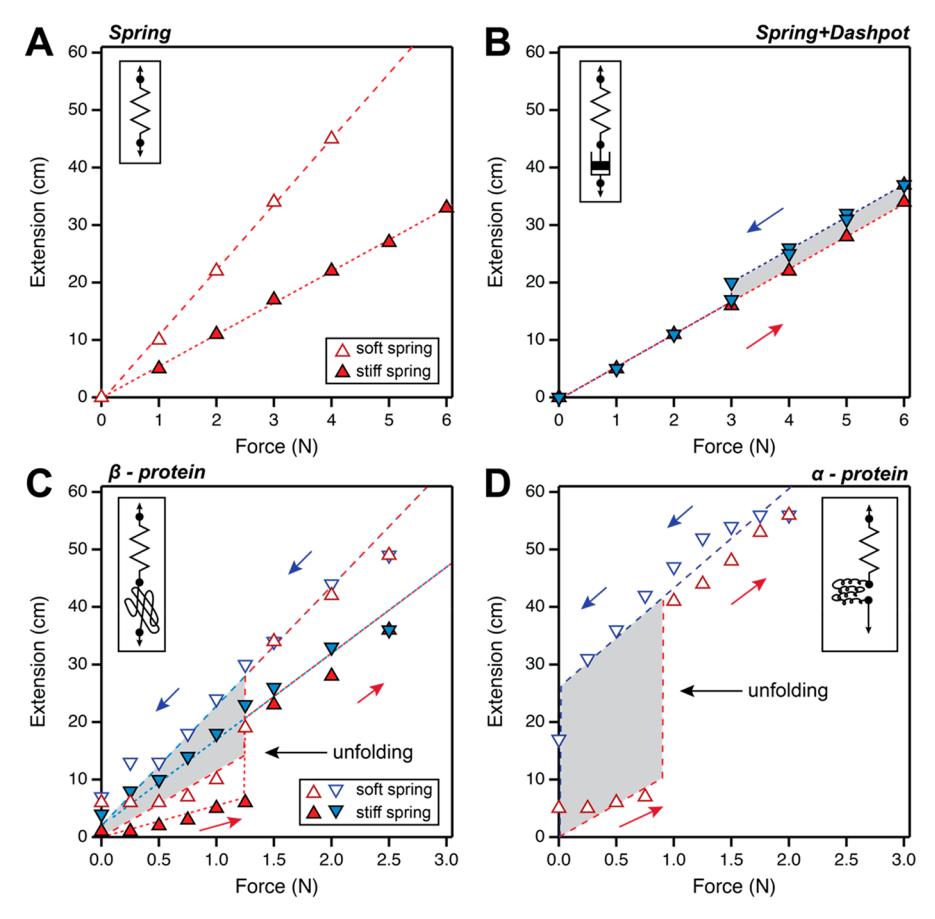


Figure 5. Data recorded for the extension as a function of force. Measured length change as a function of force for (A) two springs with different elasticities; (B) a sealed syringe in series with stiff spring; (C)  $\beta$ -protein I10 in series with a stiff and a soft spring; and (D)  $\alpha$ -protein R9 in series with a soft spring. Filled symbols were used for experiments with a stiff spring, while empty ones were used for the experiments with a soft spring. Upward pointing triangles refer to the experiments when force was increased (also denoted by the red arrows), while downward pointing triangles refer to those where force was decreased (also denoted by the blue arrows). As with real proteins, our structures also show hysteresis, with a higher unfolding than refolding force, which allows for a storage/release mechanism for mechanical energy. This hysteresis is marked with a gray area. Data were recorded from a total of N=3 experiments and represent real values expressed in Newtons and centimeters. Error bars are smaller than the markers used in the diagram.

353 3D-printed weight hanger, weighing less than 2 g (printed 354 using Tough PLA Plus from Duramic, design file available as 355 part of Supporting Information). The reason for using a lighter 356 weight hanger is that the metal weight hanger applies too much 357 force and does not allow the protein to refold back. The setup 358 also had a brown paper with markings every centimeter and 359 numbers every 10 cm, for easy reading of the extension.

Our experiment consisted of having members of the 360 audience add slotted weights and record both the extension and the force. To simplify the force readout, every 100 g of added weight was approximated to 1 N. For the first setup, as weights were added in increments of 100 g, the extension was recorded for both a soft and a stiff spring (Figure 5A). When weights were removed, the extension was recorded as well. The springs behaved the same when weights where added or subtracted, and only the points where weights were added are shown in Figure 5A. The stiff spring in our case had a spring constant of 0.18 N/cm (filled triangles), while the soft spring showed 0.09 N/cm (empty triangles). The second experiment, consisting of a spring in series with a dashpot was done only 373 with the stiff spring, as the soft spring would reach the 374 maximum extension in our setup (which was ~83 cm in total) 375 before the syringe would start to extend. As force is being 376 applied, the extension follows the same behavior as measured

for the spring alone, until a loading of 600 g. At this force, the 377 syringe plunger starts to slowly move, and after ~5 s, it reaches 378 an equilibrium point (Figure 5B). As adding more weights 379 would break the seal between the plunger and the barrel, no 380 other weights were added. When weights were subtracted, the 381 plunger showed some time delay in its response, and at 300 g is 382 fully closed. This experiment aims to explain the concept of 383 viscoelasticity. The hysteresis seen is related to the friction 384 forces developed between the rubber end of the plunger and 385 the syringe barrel. In the last experiment, a printed protein was 386 put in series with a spring (Figure 5C,D, and Movie S1 and 387 Movie S2). Smaller weights were added (25 g) to first capture 388 the extension of the spring, while the protein remained folded. 389 At a given force (125 g for I10 and 90 g for R9), the protein 390 suddenly unfolded, and after that, both the spring and the 391 unfolded structure extended together. When removing weights, 392 the extension kept decreasing without refolding of the protein 393 structure, well beyond the unfolding force. The reason here is 394 related to the fact that the magnets, while very strong, have a 395 small attractive range. In fact, for the  $\alpha$  helix protein, the 396 magnets do not come close enough to re-form the original 397 structure. There is an obvious hysteresis in our measurements, 398 as the proteins unfold at a significantly higher force than when 399 they refold. As we already know the spring constants from the 400 Journal of Chemical Education pubs.acs.org/jchemeduc Demonstration

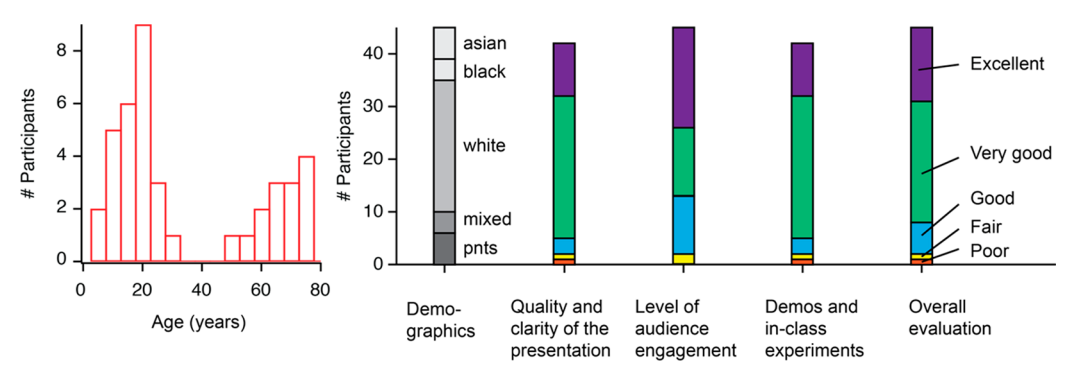


Figure 6. Summary of evaluations. (Left) Age distribution (pnts = prefer not to say). (Middle) Demographics. (Right) Program evaluations from a total of 45 evaluation forms.

401 first experiment, we can use those values to determine the 402 spring constant of the unfolded structure. To model such a 403 behavior, a second spring was added or subtracted as the force 404 increased or decreased, at the values measured experimentally 405 for (un)folding (see dotted lines in Figure 5C,D). The titin I10 406  $\beta$ -strand structure had an apparent spring constant of 0.11 N/ 407 cm in both experiments (with soft and stiff spring), while for 408 the all- $\alpha$  talin R9 structure we measured an apparent spring 409 constant of 0.17 N/cm. Several things are worth mentioning 410 here. First, the same hysteresis originating in our experiment 411 from the fact that the magnets exert a strong, but short-range 412 force, is seen for proteins, where the hydrogen bonds holding 413 the 3D structure also have a strong, but short-range, attraction 414 effect.<sup>30</sup> By having this hysteresis, proteins can effectively store 415 and dissipate important amounts of energy. This behavior is 416 also measured in tissue-like materials, where biomaterials made 417 from globular proteins show a different strain response upon 418 increasing stress and decreasing it. 32,33 However, unlike the 419 third experiment, which sees the unfolding taking place every 420 time at the same force, proteins in vivo have a probabilistic 421 behavior, and a molecule made from repeats of the same 422 protein domain will display under a constant force, with 423 unfolding steps of different time intervals.<sup>30</sup> This time-424 dependent behavior can be better related to the second 425 experiment, where viscoelastic effects introduce a time-426 dependent variable. Finally, force is a vector, and not only its 427 magnitude but also its direction are important. It is well-known 428 that the same protein pulled from different directions will show 429 vastly different unfolding kinetics. 34,35 Typically, when hydro-430 gen bonds are perpendicular to the pulling direction (known as 431 sheering geometry, which is the case for titin I10 domain), the 432 force required to unfold is higher than when hydrogen bonds 433 are parallel to the force (known as unzipping geometry, as is 434 the case for talin R9 domain). Interestingly, our experiment 435 follows this behavior, with the all- $\alpha$  structure unfolding at a 436 lower force than the all- $\beta$  structure. We note that the 437 mechanical pulling apart demonstration that we show here 438 with flexible 3D-printed structures and springs under a given 439 force actually happens at the molecular level in vivo, as detailed 440 above for talin. Obviously, the forces are much smaller 441 (picoNewtons when scaled to single proteins vs Newtons for 442 printed structures), and the extensions are proportional to the 443 protein structure (nanometers for the unfolding of a protein in 444 vivo vs millimeter extensions measured in our demonstration). 445 We also note a limitation of the 3D-printed structures having 446  $\alpha$ -helices, which in the demonstration retain the spring 447 structure after unfolding, no matter the applied force. Unlike 448 the macroscopic demonstration, the secondary structure

elements of proteins also denature at high forces, transforming 449 the protein chain into a simple polymer. 450

451

479

#### EVALUATIONS

The event was held 5 times during the month of January 2022 452 (which unfortunately coincided with one of the peaks of the 453 COVID-19 pandemic and a cold wave in Milwaukee). The 454 program was advertised through Milwaukee and Shorewood 455 public schools and recreation departments, as well as through 456 social media such as Twitter, Facebook, etc. The event was 457 attended by a total of 143 people. Members of the audience 458 were actively involved in the experiments described above and 459 were rewarded with 3D-prints of the proteins from Figure 3. 460 Evaluation forms were designed following standard templates 461 from surveymonkey.com and personalized for this event. 462 Evaluation forms were distributed one-per-group (family) and 463 left at end of the event in an unattended box. The answers to 464 the questions are summarized in Figure 6. We saw a bimodal 465 f6 distribution of age, with 55% of the self-reporting members of 466 the audience being of K-12 age. This bimodal distribution 467 reflects that smaller children were typically accompanied by 468 their parents or grandparents. The demographics from those 469 who reported on the question about race show an attendance 470 of 44% from minority (26% from underrepresented minorities 471 in science), above the Wisconsin demographics (which is 18% 472 for minorities and 15% for under-represented minorities, 473 according to census data from 2021 https://www.census.gov/ 474 quickfacts/WI). All the questions on the evaluation of the 475 quality of the event were over 50% rated as "Very good" or 476 "Excellent", with the assessment on the level of engagement 477 having the highest proportion of "Excellent" rankings.

## CONCLUSIONS

We have described a set of experiments that have been 480 successfully implemented in an open-public event and can 481 constitute an improved learning experience for students being 482 taught protein folding. The experiments shown use inexpensive 483 magnets and take advantage of the large availability and 484 increased affordability of 3D-printing technology. Several 485 simple structures printed from materials that reflect the *in* 486 *vivo* properties of proteins are demonstrated in this study. 487 Furthermore, structures printed in a flexible material were used 488 to demonstrate a profound behavior of mechanical unfolding 489 of proteins and relate it to macroscopic changes on how cells 490 and tissues respond. During this event, we learned that direct 491 involvement of the audience increases both their attention and 492 their understanding. A challenge came from the time needed to

551

558

494 print the 3D structures. While only costing less than a quarter 495 in material, the time needed for printing and cleaning of each 496 structure was ~3.5 h. Furthermore, generating removable tree-497 supports allowed us to print protein structures without any 498 artificial linking parts. While the demonstrations presented 499 here were done as part of an outreach event, they could easily 500 be incorporated into a course, as most high schools and 501 universities have access to 3D-printers. Another demonstration 502 could also come from having students identify a protein 503 structure and follow the instructions in the manuscript to 3D-504 print that structure. The approach presented here will help 505 visual learners by allowing students to physically interact with 506 protein structures that are large enough to be held in their 507 hands. Furthermore, by combining experiments on spring 508 elasticity and dashpot response, that are typically encountered 509 in mechanics laboratories, with unfolding of flexible protein 510 structures, students can better understand how proteins 511 operate in vivo under a force to change their extension. 512 Obviously, the demonstrations provided here have the 513 potential to improve engagement and interest in a classroom 514 setting. We envision the use of hands-on demonstrations as a 515 successful approach to teach students about the wonders of 516 science.

## 517 **ASSOCIATED CONTENT**

## 18 Supporting Information

519 The Supporting Information is available at https://pubs.ac-520 s.org/doi/10.1021/acs.jchemed.2c00231.

File to use as weight hangar .stl upon changing the extension from .txt to .stl (TXT)

Additional figures showing hydrophobic collapse during protein folding and various representations of proteins (PDF)

File to use as syringe plunger .stl upon changing the extension from .txt to .stl (TXT)

Movie S1 showing extension and contraction of a spring (MP4)

Movie S2 showing extension and contraction of a spring in series with a dashpot (MP4)

Movie S3 showing unfolding and refolding of a  $\beta$ -protein (MP4)

Movie S4 showing unfolding and refolding of an  $\alpha$ protein (MP4)

Weight hanger and syringe plunger .stl files (ZIP)

### **537 AUTHOR INFORMATION**

#### 38 Corresponding Author

Ionel Popa – Department of Physics, University of
Wisconsin—Milwaukee, Milwaukee, Wisconsin 53211,
United States; orcid.org/0000-0003-3111-4716;
Email: popa@uwm.edu

#### 543 Author

Florin Saitis – Department of Physics, University of Wisconsin—Milwaukee, Milwaukee, Wisconsin 53211, United States

547 Complete contact information is available at: 548 https://pubs.acs.org/10.1021/acs.jchemed.2c00231

#### 549 Notes

550 The authors declare no competing financial interest.

#### ACKNOWLEDGMENTS

We acknowledge Michael Gerard Condon from the UWM 552 Physics Machine Shop for helping us to assemble the 553 demonstration setups and Naomi Raicu, Suha Malik, Christine 554 Wiley, Norman P. Lasca, and L&S UWM, for organizing the 555 event. This study was funded by National Science Foundation 556 (MCB-1846143 and DBI-1919670).

#### REFERENCES

- (1) Alberts, B.; Johnson, A.; Lewis, J.; Raff, M.; Roberts, K.; Walter, 559 P. *Molecular Biology of the Cell*, 6th ed.; Garland Publishing: New 560 York, 2002.
- (2) Dill, K. A.; MacCallum, J. L. The protein-folding problem, 50 562 years on. *Science* **2012**, 338 (6110), 1042–6.
- (3) Levinthal, C. Are there pathways for protein folding? *J. Chem.* 564 *Phys.* **1968**, 65, 44–45.
- (4) Popa, I.; Berkovich, R. Mechanobiology: protein refolding under 566 force. Emerg. Top. Life Sci. 2018, 2 (5), 687–699.
- (5) Lin, M. M.; Zewail, A. H. Protein folding simplicity in 568 complexity. *Annalen der Physik* **2012**, 524 (8), 379–391.
- (6) Baldwin, R. L.; Frieden, C.; Rose, G. D. Dry molten globule 570 intermediates and the mechanism of protein unfolding. *Proteins* **2010**, 571 78 (13), 2725–37.
- (7) Sharma, S.; Subramani, S.; Popa, I. Does protein unfolding play a 573 functional role in vivo? *FEBS J.* **2021**, 288 (6), 1742–1758.
- (8) del Rio, A.; Perez-Jimenez, R.; Liu, R.; Roca-Cusachs, P.; 575 Fernandez, J. M.; Sheetz, M. P. Stretching single talin rod molecules 576 activates vinculin binding. *Science* **2009**, 323 (5914), 638–41.
- (9) Popa, I.; Gutzman, J. H. The extracellular matrix—myosin 578 pathway in mechanotransduction: from molecule to tissue. *Emerg.* 579 *Top. Life Sci.* **2018**, 2 (5), 727–737.
- (10) Kontra, C.; Lyons, D. J.; Fischer, S. M.; Beilock, S. L. Physical 581 experience enhances science learning. *Psychol. Sci.* **2015**, *26* (6), 737–582 49.
- (11) Bruce, M. R. M.; Bruce, A. E.; Bernard, S. E.; Bergeron, A. N.; 584 Ahmad, A. A. L.; Bruce, T. A.; Perera, D. C.; Pokhrel, S.; Saleh, S.; 585 Tyrina, A.; Yaparatne, S. Designing a Remote, Synchronous, Hands-586 On General Chemistry Lab Course. *J. Chem. Educ.* **2021**, 98 (10), 587 3131–3142.
- (12) Pernaa, J.; Wiedmer, S. A systematic review of 3D printing in 589 chemistry education analysis of earlier research and educational use 590 through technological pedagogical content knowledge framework. 591 Chemistry Teacher International 2020, 2 (2), 20190005.
- (13) Alimi, O. A.; Meijboom, R. Current and future trends of 593 additive manufacturing for chemistry applications: a review. *J. Mater.* 594 *Sci.* **2021**, *56* (30), 16824–16850.
- (14) Renner, M.; Griesbeck, A. Think and Print: 3D Printing of 596 Chemical Experiments. J. Chem. Educ. 2020, 97 (10), 3683–3689.
- (15) Martínez, L. Introducing the Levinthal's Protein Folding 598 Paradox and Its Solution. *J. Chem. Educ.* **2014**, 91 (11), 1918–1923. 599 (16) Scaletti, C.; Rickard, M. M.; Hebel, K. J.; Pogorelov, T. V.; 600 Taylor, S. A.; Gruebele, M. Sonification-Enhanced Lattice Model 601
- Animations for Teaching the Protein Folding Reaction. *J. Chem. Educ.* 602 **2022**, 99 (3), 1220–1230. 603 (17) Prigozhin, M. B.: Scott, G. E.: Denos, S. Mechanical Modeling 604
- (17) Prigozhin, M. B.; Scott, G. E.; Denos, S. Mechanical Modeling 604 and Computer Simulation of Protein Folding. *J. Chem. Educ.* **2014**, 91 605 (11), 1939–1942.
- (18) Carlson, T. M.; Lam, K. W.; Lam, C. W.; He, J. Z.; Maynard, J. 607 H.; Cavagnero, S. Naked-Eye Detection of Reversible Protein Folding 608 and Unfolding in Aqueous Solution. *J. Chem. Educ.* **2017**, *94* (3), 609 350–355.
- (19) Franco, J. Online Gaming for Understanding Folding, 611 Interactions, and Structure. *J. Chem. Educ.* **2012**, 89 (12), 1543–1546. 612 (20) Meyer, S. C. 3D Printing of Protein Models in an 613 Undergraduate Laboratory: Leucine Zippers. *J. Chem. Educ.* **2015**, 614 92 (12), 2120–2125.

Journal of Chemical Education

- 616 (21) Jones, O. A. H.; Spencer, M. J. S. A Simplified Method for the 617 3D Printing of Molecular Models for Chemical Education. *J. Chem.* 618 Educ. **2018**, 95 (1), 88–96.
- 619 (22) Da Veiga Beltrame, E.; Tyrwhitt-Drake, J.; Roy, I.; Shalaby, R.; 620 Suckale, J.; Pomeranz Krummel, D. 3D Printing of Biomolecular 621 Models for Research and Pedagogy. *JoVE* **2017**, No. 121, e55427.
- 622 (23) Akerstrom, B.; Bjorck, L. Protein L: an immunoglobulin light
- 623 chain-binding bacterial protein. Characterization of binding and
- 624 physicochemical properties. J. Biol. Chem. 1989, 264 (33), 19740-6.
- 625 (24) Crampton, N.; Alzahrani, K.; Beddard, G. S.; Connell, S. D.;
- 626 Brockwell, D. J. Mechanically Unfolding Protein L Using a Laser-
- 627 Feedback-Controlled Cantilever. *Biophys. J.* **2011**, *100* (7), 1800–628 1809.
- 629 (25) Valle-Orero, J.; Rivas-Pardo, J. A.; Popa, I. Multidomain 630 proteins under force. *Nanotechnology* **2017**, 28 (17), 174003.
- 631 (26) Dahal, N.; Nowitzke, J.; Eis, A.; Popa, I. Binding-Induced
- 632 Stabilization Measured on the Same Molecular Protein Substrate
- 633 Using Single-Molecule Magnetic Tweezers and Heterocovalent 634 Attachments. J. Phys. Chem. B 2020, 124 (16), 3283–3290.
- 635 (27) Sprague-Piercy, M. A.; Rocha, M. A.; Kwok, A. O.; Martin, R.
- 636 W. α-Crystallins in the Vertebrate Eye Lens: Complex Oligomers and 637 Molecular Chaperones. *Annu. Rev. Phys. Chem.* **2021**, 72 (1), 143–638 163.
- 639 (28) Eckels, E. C.; Tapia-Rojo, R.; Rivas-Pardo, J. A.; Fernandez, J. 640 M. The Work of Titin Protein Folding as a Major Driver in Muscle 641 Contraction. *Annu. Rev. Physiol.* **2018**, *80*, 327–351.
- 642 (29) Chalfie, M.; Tu, Y.; Euskirchen, G.; Ward, W. W.; Prasher, D.
- 643 C. Green Fluorescent Protein as a Marker for Gene-Expression. 644 Science 1994, 263 (5148), 802-805.
- 645 (30) Popa, I.; Rivas-Pardo, J. A.; Eckels, E. C.; Echelman, D. J.;
- 646 Badilla, C. L.; Valle-Orero, J.; Fernandez, J. M. A HaloTag Anchored
- 647 Ruler for Week-Long Studies of Protein Dynamics. *J. Am. Chem. Soc.* 648 **2016**, 138 (33), 10546–53.
- 649 (31) Freundt, J. K.; Linke, W. A. Titin as a force-generating muscle 650 protein under regulatory control. *J. Appl. Physiol.* **2019**, *126* (5), 651 1474–1482.
- 652 (32) Khoury, L. R.; Nowitzke, J.; Shmilovich, K.; Popa, I. Study of
- 653 Biomechanical Properties of Protein-Based Hydrogels Using Force-
- 654 Clamp Rheometry. *Macromolecules* **2018**, *51* (4), 1441–1452.
- 655 (33) Shmilovich, K.; Popa, I. Modeling Protein-Based Hydrogels
- 656 under Force. Phys. Rev. Lett. 2018, 121 (16), 168101.
- 657 (34) Sikora, M.; Cieplak, M. Mechanical stability of multidomain 658 proteins and novel mechanical clamps. *Proteins: Struct. Funct. Genet.*
- 659 **2011**, 79 (6), 1786–1799.
- 660 (35) Guo, S. W.; Efremov, A. K.; Yan, J. Understanding the catch-
- 661 bond kinetics of biomolecules on a one-dimensional energy landscape.
- 662 Commun. Chem. 2019, 2, 30.